Available online at www.sciencedirect.com
SCIENCE DIRECT
Engineering Structures 28 (2006) 503–513
ENGINEERING STRUCTURES
www.elsevier.com/locate/engstruct

# Wind-induced response and serviceability design optimization of tall steel buildings

C.-M. Chan*, J.K.L. Chui

*Department of Civil Engineering, Hong Kong University of Science and Technology, Kowloon, Hong Kong, China*

Received 3 June 2004; received in revised form 31 August 2005; accepted 3 September 2005
Available online 17 October 2005

**Abstract**

Trends towards constructing taller and increasingly slender buildings imply that these structures are potentially more responsive to wind excitation, causing discomfort to occupants. This paper seeks to develop an integrated wind tunnel load analysis and automatic least cost design optimization procedure to assist structural engineers in the prediction of wind-induced response based on the High Frequency Force Balance (HFFB) technique and on the serviceability design of tall steel buildings. It has been shown that the wind-induced acceleration is inversely related to the natural frequency of tall buildings within the range of frequency for serviceability checking. An Optimality Criteria (OC) method is developed to minimize the structural cost of steel buildings subject to targeted frequency constraints in which the limiting frequency threshold is derived from the motion perception design criteria of ISO Standard 6897. The effectiveness of the proposed integrated wind tunnel analysis and numerical design optimization procedure is illustrated through a full-scale 45-story symmetric tubular steel building example. This building was initially found to vibrate excessively under wind loading and then the automated optimization procedure was used to determine the optimal structural stiffness satisfying the stipulated ISO Standard 6897 occupant comfort criteria.


*Keywords:* Wind-induced vibration; Motion perception; Serviceability design; Structural optimization; Tall buildings

## 1. Introduction

Recent trends towards constructing increasingly slender and taller buildings, with higher strength materials and lighter structural systems, have contributed to a new generation of wind-sensitive buildings. Very often, such slender and tall buildings experience excessive wind-induced vibration, which will cause discomfort to occupants or even shatter windows, raising concerns about serviceability design problems [1–3]. It has been widely accepted that the perception of wind-induced motion is closely related to the acceleration of buildings [1]. The wind loads on a building are very dependent on the building's shape, height, and surroundings. Most wind codes and standards derived based on simple geometric building shapes are incapable of accurately predicting wind loads and their effects on modern buildings of unusual shapes. For the past 30 years, wind-tunnel testing has become the best practice in estimating wind effects on tall buildings. The High Frequency Force Balance (HFFB) technique is often used to determine the wind forces acting on buildings [4]. In this approach, a lightweight rigid model of the structure is mounted on a very stiff base balance capable of measuring aerodynamic loads over a range of incidence angles of the approaching wind. A major advantage of this approach is that wind force spectra can be measured directly while taking into account the wind buffeting caused by surrounding buildings or the terrain. Once the wind force spectra derived from the HFFB technique are obtained, they can be used to predict the lateral drift and acceleration responses analytically using the random vibration theory. As long as the geometric configuration of the building does not change, the same set of wind force spectra can be used to estimate the effects of structural design modifications without the need for further wind-tunnel tests [5]. Further details and recent advancements of various wind tunnel techniques can be referred to reference [6].

Although well-established aerodynamic and aeroelastic wind-tunnel techniques have been developed for accurate

* Corresponding author. Tel.: +852 2358 7173; fax: +852 2358 1534.
*E-mail address:* cecmchan@ust.hk (C.-M. Chan).

0141-0296/$ - see front matter © 2005 Elsevier Ltd. All rights reserved.
doi:10.1016/j.engstruct.2005.09.005

prediction of wind forces and wind-induced responses of tall buildings, a systematic design optimization technique for economical design of tall buildings subject to wind-induced serviceability design performance requirements is still lacking. Attempts were made in the past to control the wind-induced motion of tall steel buildings under wind excitation. Kwok et al. [7,8] studied the effects of chamfered corners and slotted corners of prismatic tall buildings on the wind-induced responses of such buildings. Although they showed that chamfers on the order of 10% of the building's width may result in 30% to 40% reduction in both alongwind- and crosswind-induced motions of tall buildings, engineers are usually unable to change the building's shape, which is normally defined and determined by the architect. In the last decade, much research effort [9–11] has been put into structural control, leading to the concept of using various structural damping devices with different kinds of control strategies, to reduce the wind-induced motion of tall buildings. Although structural damping devices have been theoretically found to be very effective to mitigate the problems of excessive wind-induced vibration and there have been some remarkable applications in Japan [12], the use of structural control can hardly become widely accepted in today's building construction. The long-term reliability issues, operation and maintenance costs, as well as higher initial installation cost of structural control systems have raised serious questions on the practicality and cost-effectiveness of such devices.

While adding mechanical dampers and modifying the aerodynamic shapes and properties of tall buildings are not always considered realistic and feasible, the design of an appropriate structural system seems to be the most practical way for the structural engineers to suppress wind-induced motion in tall buildings. It has long been realized that the acceleration response of wind-sensitive buildings is generally inversely related to the building's stiffness within the range of frequency for serviceability checking [2,3]. In the case of slender tall buildings, the crosswind vortex shedding motion is widely accepted to be the most critical wind-induced response. This is the well-known resonance effect caused by the coincidence of the vortex shedding frequency and the natural frequency of a building. Therefore, designing an appropriate stiffness for a building while moving the building's natural frequency away from the vortex shedding frequency, especially in the crosswind direction, can effectively reduce the amount of wind excitation energy received by the building, resulting in a subsequent reduction in wind-induced acceleration. Indeed, Tallin and Ellingwood [2] have demonstrated the effect of increasing the structure's stiffness on suppressing excessive wind-induced motion in a generic symmetric square building example. From their results, increasing the natural frequency from 0.15 to 0.30 Hz while keeping the mass constant can effectively reduce the crosswind response by two-thirds.

Practicing engineers rely heavily on experience and intuition in the design of tall buildings against wind excitation. It is generally not an easy task to develop an economical structural system for tall buildings with the desired stiffness and satisfactory occupant comfort performance while ensuring the optimum distribution of structural material. While a building's mass is kept unchanged, the lateral stiffness of the building can be directly related to the natural frequency of the building. In this paper, the Optimality Criteria (OC) method, which has been widely used in the aerospace industry [13] and shown to be very effective in lateral drift design of tall buildings [14–17], will be extended to minimize the cost of tall symmetric steel buildings subject to wind-induced acceleration performance constraints expressed in terms of the natural frequency of the building. In this approach, a set of necessary optimality conditions for the optimal design is first derived and a recursive algorithm is then applied to search for the optimal design indirectly by satisfying the set of optimality conditions. The illustrative example is a 45-story symmetric tubular steel building, initially found to have excessive wind-induced vibration. Using the proposed integrated wind tunnel analysis and the Optimality Criteria method, the steel framework can be stiffened with the most cost effective element stiffness distribution, while achieving satisfactory wind-induced acceleration performance according to the stipulated ISO Standard 6897 [18] occupant comfort requirements.

## 2. The aerodynamic wind tunnel technique

The High Frequency Force Balance (HFFB) technique has been widely used to determine the wind loads and wind-induced acceleration of buildings. This technique combines both theoretical analysis and experimental results to synthesize the loads and responses of buildings under wind excitation. When compared to the traditional aeroelastic modeling technique, which requires complete modeling of the dynamic properties of the building, the HFFB method is less expensive and more efficient since it requires only the proper modeling of the exterior geometric shape of the building in a simulated boundary layer flow.

From the classical modal analysis, the equation of motion can be stated as:

$$m_j \ddot{x}_j + c_j \dot{x}_j + k_j x_j = F_j \tag{1}$$

where $m_j$ is the modal mass; $c_j$ is the modal damping; $k_j$ is the modal stiffness; $x_j$ is the modal amplitude; $F_j$ is the modal wind force, which can be measured by HFFB; $j$ is the mode number.

In the structural design of most tall symmetric buildings, only the fundamental modes in the alongwind and crosswind directions will be considered. These wind directions are usually associated with the first two modes of the building. Indeed, higher mode effects are generally negligible in wind engineering design [19]. Note that only tall symmetrical buildings are considered in this paper, mode shape corrections are necessary for asymmetrical buildings with nonlinear and coupled mode shapes when using the HFFB technique [20]. Once the wind modal force spectra are measured, the equation of motion in Eq. (1) can be solved using the classical random vibration theory in the frequency domain. The spectra of the wind-induced acceleration can be calculated by multiplying

the square of the mechanical admittance function by the wind modal force spectra:

$$S_{a_j}(n) = |H_j(n)|^2 S_{Fj}(n) \tag{2}$$

where the mechanical admittance function is defined as

$$|H_j(n)|^2 = \frac{(2\pi n)^4}{[1-(n/n_j)^2]^2 + [2\xi_j n/n_j]^2} \tag{3}$$

in which $n_j$ is the $j$th mode frequency and $\xi_j$ is the $j$th mode damping ratio. $S_{a_j}(n)$ provides a statistical description of the $j$th modal acceleration response; however, it is often the root mean square value of the wind-induced acceleration that provides useful information for the design of the buildings. By integrating the area underneath the acceleration spectra, the mean square value of the wind-induced acceleration can then be calculated as:

$$\ddot{\sigma}_{a_j}^2 = \int_0^\infty S_{a_j}(n)\,\mathrm{d}n = \int_0^\infty |H_j(n)|^2 S_{Fj}(n)\,\mathrm{d}n. \tag{4}$$

Although the wind force spectrum, $S_{Fj}(n)$, is usually broad band, modern tall buildings, being usually lightly damped, behave like a narrow band filter, thus leading to the results of narrow band acceleration output. Assuming that $S_{Fj}(n)$ is white noise in Eq. (4), the resonance part of the root mean square acceleration response can then be approximated as:

$$\ddot{\sigma}_{a_j} = \sqrt{S_{Fj}(n_j)\int_0^\infty |H_j(n)|^2\,\mathrm{d}n} \cong \sqrt{\frac{\pi n_j S_{Fj}(n_j)}{4\xi_j m_j^2}}. \tag{5}$$

## 3. Dependence of wind-induced acceleration on natural frequency of structure

From Eq. (5), it seems apparent that the mean square acceleration is directly proportional to the frequency of the building. As a matter of fact, when the relationship of the spectral density $S_{Fj}(n_j)$ is explicitly expressed in terms of $n_j$, as shown later for the CAARC building, $S_{Fj}(n_j)$ is actually found to be so inversely related to the frequency that the product term $n_j S_{Fj}(n_j)$ actually becomes also inversely related to the frequency. Studies by Tallin and Ellingwood [2] and Griffis [3] have shown that tall buildings are generally found within the frequency range of 0.1–1.0 Hz in which the power spectral density of the wind-induced acceleration is inversely proportional to the natural frequency. In other words, within the range of frequency for the serviceability check, the wind force and subsequently the acceleration response of a tall building can normally be reduced by increasing the natural frequency of the building.

Fig. 1 presents a series of alongwind and crosswind force spectra for rectangular tall buildings of various height-to-width aspect ratios in an urban environment. These spectra are reproduced from the aerodynamic load database of the NatHaz Modeling Laboratory at the URL address http://www.nd.edu/~nathaz/database/index.html [21]. As illustrated clearly in Fig. 1, the power spectral density of wind force attenuates rapidly with increasing frequency when the reduced frequency ($nB/V_H$) is larger than 0.1. Simple empirical expressions now exist in the literature as well as various codes and standards that allow approximate evaluation of wind-induced acceleration responses to wind action [22–25]. Similar expressions for the alongwind, crosswind and torsional RMS acceleration of a square building in an urban environment have been presented in terms of wind velocity, mass, stiffness and damping by Islam et al. [22]. Vickery et al. [23] indicated that an increase in the stiffness is advantageous especially in the event of controlling crosswind vortex shedding of a tall building.

In order to illustrate the relationships between wind-induced acceleration and natural frequency, an example building with the geometric shape of the CAARC standard building [26] with plan dimensions of 30 m by 45 m and a height of 180 m is considered. Two perpendicular wind directions in an urban boundary layer have been considered in this example: (1) wind coming along the X-direction where $B = 30$ m and (2) wind coming along the Y-direction where $B = 45$ m. The aerodynamic wind force spectra derived from wind tunnel testing can be directly downloaded from the NatHaz aerodynamic loads database. Due to the fact that the wind force spectra are given in a logarithmic format, they can be written explicitly in the form of exponential natural frequency functions via regression analysis, within the range of reduced frequency for serviceability checking where $nB/V_H > 0.1$ [22,24].

For the approaching wind in the long direction of the CAARC standard building (i.e., in the X-direction where $B = 30$ m), the wind force spectra within the range of reduced frequency for the serviceability check can be approximated as:

$$\text{Alongwind:}\quad n_x S_{F_x} = 141.543 \times 10^6 n_x^{-1.363}\ (\mathrm{N}^2),\quad \left(\frac{n_x B}{V_H}\right) \geq 0.1 \tag{6a}$$

$$\text{Crosswind:}\quad n_y S_{F_y} = 26.556 \times 10^6 n_y^{-3.027}\ (\mathrm{N}^2),\quad \left(\frac{n_y B}{V_H}\right) \geq 0.1. \tag{6b}$$

When the approaching wind is acting in the short direction (i.e., in the Y-direction where $B = 45$ m), the wind force spectra can be approximated as:

$$\text{Alongwind:}\quad n_y S_{F_y} = 90.143 \times 10^6 n_y^{-2.019}\ (\mathrm{N}^2),\quad \left(\frac{n_y B}{V_H}\right) \geq 0.1 \tag{7a}$$

$$\text{Crosswind:}\quad n_x S_{F_x} = 36.362 \times 10^6 n_x^{-2.841}\ (\mathrm{N}^2),\quad \left(\frac{n_x B}{V_H}\right) \geq 0.1. \tag{7b}$$

Assuming a building density of 125 kg/m$^3$, a damping ratio of 1% and a 5-year return period hourly mean design wind speed, $V_H$, of 25 m/s at the top of the building, the root mean square acceleration response at the top of the building can then be expressed solely in terms of the natural frequency by substituting Eqs. (6) and (7) respectively into Eq. (5) as

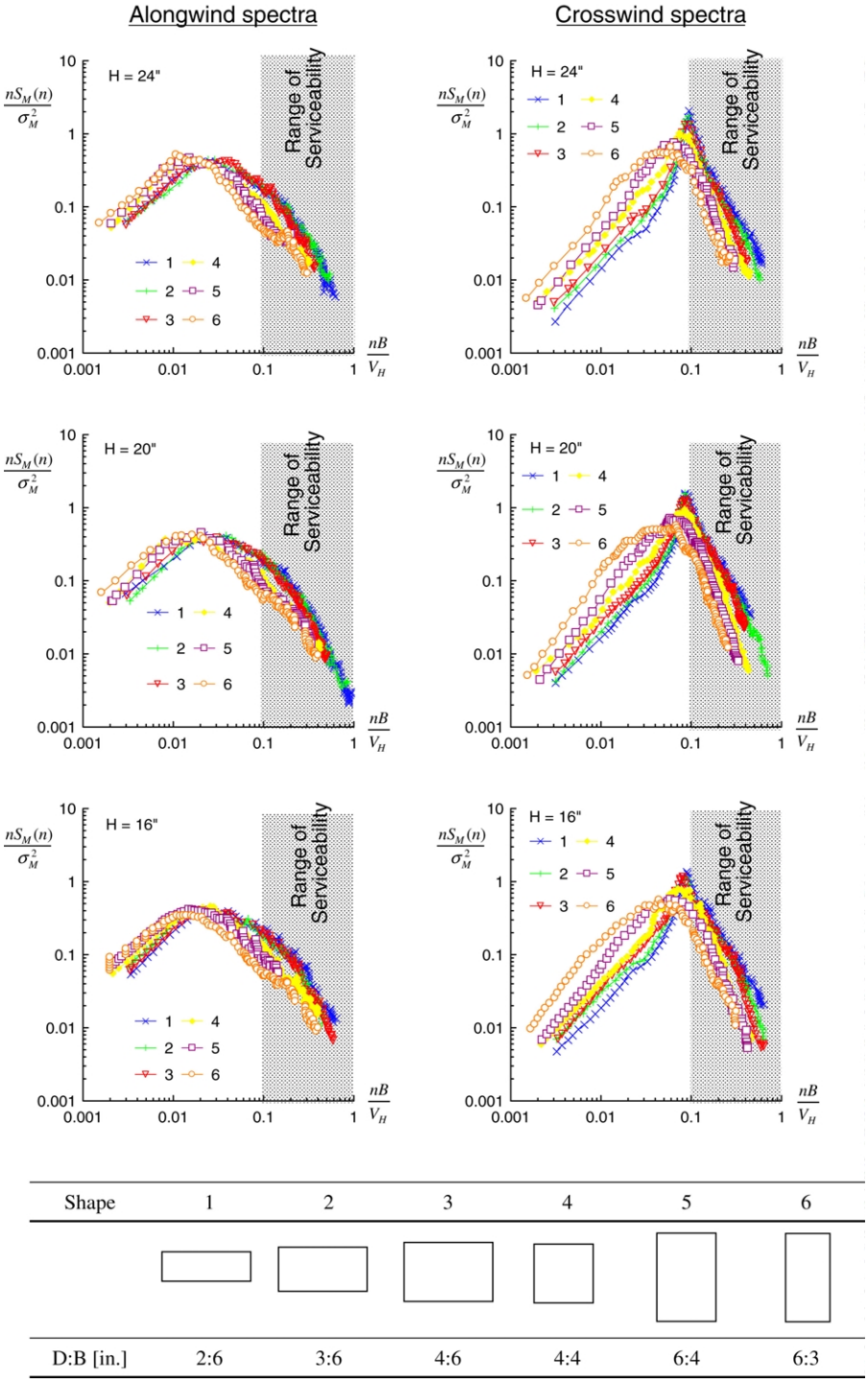


Fig. 1. Typical alongwind and crosswind aerodynamic base moment spectra.

For approaching wind in the X-direction ($B = 30$ m):

Alongwind RMS acceleration:

$$\ddot{\sigma}_{a_x} = 10.075 \times 10^{-3} n_x^{-0.682} \ (\mathrm{m/s^2}) \tag{8a}$$

Crosswind RMS acceleration:

$$\ddot{\sigma}_{a_y} = 4.364 \times 10^{-3} n_y^{-1.513} \ (\mathrm{m/s^2}). \tag{8b}$$

For approaching wind in the Y-direction ($B = 45$ m):

Alongwind RMS acceleration:

$$\ddot{\sigma}_{a_y} = 8.040 \times 10^{-3} n_y^{-1.000} \ (\mathrm{m/s^2}) \tag{9a}$$

Crosswind RMS acceleration:

$$\ddot{\sigma}_{a_x} = 5.107 \times 10^{-3} n_x^{-1.420} \ (\mathrm{m/s^2}). \tag{9b}$$

As clearly shown in Eqs. (8a), (8b) and Eqs. (9a), (9b), the wind-induced acceleration of the building example is given as a negative exponential function of the building's frequency. Therefore, increasing the natural frequency of the building will cause a reduction in both the alongwind and crosswind

acceleration responses of the building. Although Eqs. (8a), (8b) and (9a), (9b) were derived mainly for use in the case of the CAARC building, experience has shown that similar results of the relationships between the wind-induced acceleration and the natural frequency are generally found for typical tall buildings. Similar sets of expressions for RMS acceleration have also been derived for square, symmetric tall buildings in reference [3]. Fig. 1 also shows graphically that the power density of wind force is generally found to attenuate rapidly with increasing frequency within the typical range of tall buildings. In general, when comparing the alongwind acceleration with the crosswind acceleration, a stronger dependence of the crosswind acceleration on a building's frequency is found. Once the explicit relationships between the wind induced acceleration and the natural frequencies of a building are established, the targeted minimum frequencies of the building can then be determined based on certain acceptable occupant comfort design criteria. In this study, the following ISO Standard 6897 acceleration perception threshold for low frequency horizontal motion is considered:

$$\ddot{\sigma}_a = \exp(-3.65 - 0.41 \ln n). \tag{10}$$

Note that the ISO Standard 6897 acceleration threshold value is also written as a function of the natural frequency of a building. Therefore, balancing the acceleration response functions given in Eqs. (8) and (9) with the acceleration threshold function of ISO Standard 6897 in Eq. (10) will then produce a set of minimum frequency targets. As a result, the design problem of suppressing wind-induced acceleration in tall buildings can be practically reduced to the problem of controlling the natural frequency while the damping and the mass of the building are instantaneously kept constant.

## 4. Design optimization

Although it has been recognized that increasing the natural frequency of a tall building can considerably reduce the wind-induced acceleration, direct and efficient methods for optimally sizing and stiffening tall building structures to achieve the desired frequency targets are still lacking. One main goal of this paper is to develop a numerical optimization technique to automate the element stiffness design of tall steel building structures subject to multiple frequency design constraints.

### 4.1. Design problem formulation

Consider a steel framework of a given geometry having $i = 1, 2, \ldots, N$ members (or member fabrication groups) with the cross-sectional area of each member a design variable. The design optimization problem can be stated to minimize the structural cost of the steel framework subject to multiple natural frequency constraints as:

$$\text{Minimize} \quad W(a_i) = \sum_{i=1}^{N} w_i a_i \tag{11a}$$

Subject to

$$n_j^L \le n_j \quad (j = 1, 2, \ldots, M) \tag{11b}$$

$$a_i^L \le a_i \le a_i^U \quad (i = 1, 2, \ldots, N) \tag{11c}$$

where $a_i$ is the cross-sectional area of member $i$; $w_i$ is the cost coefficient associated with the member; $a_i^L$ and $a_i^U$ define the respective lower and upper size bounds for the member. Eq. (11b) defines the set of $j = 1, 2, \ldots, M$ frequency constraints in which the current $j$th modal frequency, $n_j$, of the building is required to be greater than its specified minimum target frequency, $n_j^L$. In order to facilitate a computer solution of the design optimization problem, it is necessary that the frequency constraints be expressed explicitly in term of the sizing design variable, $a_i$, as described in the following section.

### 4.2. Explicit formulation of frequency constraints

By the Rayleigh Quotient method, the angular frequency of a structure can be given as:

$$\omega^2 = (2\pi n)^2 = \frac{\frac{1}{2}\phi^{\mathrm{T}} K \phi}{\frac{1}{2}\phi^{\mathrm{T}} M \phi} = \frac{K^*}{M^*} \tag{12}$$

where $K, K^*$ are the structure's stiffness and modal stiffness; $M, M^*$ are the structure's mass and modal mass and $\phi$ is the mode shape under the inertia force.

By conservation of energy of an undamped building structure, the total external work done by inertia forces must be equal to the total internal strain energy, $U$, stored in each structural element of the building. For a skeletal steel building framework, the total internal strain energy can be obtained by summing up the work done on each member as:

$$U = \frac{1}{2}\sum_{i=1}^{N}\int_0^{L_i}\left(\frac{F_x^2}{Ea} + \frac{F_y^2}{GA_y} + \frac{F_z^2}{GA_z} + \frac{M_x^2}{GI_x} + \frac{M_y^2}{EI_y} + \frac{M_z^2}{EI_z}\right)_i \mathrm{d}x \tag{13}$$

where $L_i$ is the length of member $i$; $F_x$, $F_y$, $F_z$, $M_x$, $M_y$, and $M_z$ are the internal frame element forces and moments due to the modal inertia loading; $E$ and $G$ are the Young's modulus and shear modulus of the steel material; $a$, $A_y$, $A_z$ are the axial and shear areas and $I_x$, $I_y$, $I_z$ are the torsional and flexural moments of inertia of each member. Previous studies by Chan [17] have shown that the shear areas ($A_y$, $A_z$) and moments of inertia ($I_x$, $I_y$, $I_z$) of standard steel sections can be related to the cross-sectional area, $a_i$, by the following reciprocal relationships:

$$1/A_y = C_{Ay}(1/a) + C'_{Ay}; \tag{14a}$$

$$1/A_z = C_{Az}(1/a) + C'_{Az} \tag{14b}$$

$$1/I_x = C_{Ix}(1/a) + C'_{Ix}; \tag{14c}$$

$$1/I_y = C_{Iy}(1/a) + C'_{Iy} \tag{14d}$$

$$1/I_z = C_{Iz}(1/a) + C'_{Iz} \tag{14e}$$

where the $C$ and $C'$ are proportionality constants determined by regression analysis depending on the shape and type of the standard steel sections. By substituting the cross-sectional relationships in Eqs. (14a)–(14e), the total internal strain energy, $U$, in Eq. (13) can be expressed concisely in terms of

the independent sizing design variable, $a_i$, as:

$$U(a_i) = \sum_{i=1}^{N} \left( \frac{e_i}{a_i} + e_i' \right) \tag{15a}$$

in which

$$e_i = \int_0^{L_i} \left( \frac{F_x^2 + M_y^2 C_{Iy} + M_z^2 C_{Iz}}{E} + \frac{F_y^2 C_{Ay} + F_z^2 C_{Az} + M_x^2 C_{Ix}}{G} \right)_i \mathrm{d}x \tag{15b}$$

$$e_i' = \int_0^{L_i} \left( \frac{M_y^2 C'_{Iy} + M_z^2 C'_{Iz}}{E} + \frac{F_y^2 C'_{Ay} + F_z^2 C'_{Az} + M_x^2 C'_{Ix}}{G} \right)_i \mathrm{d}x. \tag{15c}$$

Assume that the internal element forces and moments due to the modal inertia loading given in Eqs. (15b) and (15c) are instantaneously kept constant. From Eq. (15a), it can be recognized that increasing the element sizes will lead to an increase in the structure's stiffness and result in a reduction in the total internal strain energy, $U$. In other words, the structure's stiffness is inversely proportional to the total internal strain energy, $U$. If the structure's stiffness is to be increased, it can also be observed from Eq. (12) that there will be a subsequent increase in the frequency of the structure. As a result, one may deduce that the total internal strain energy, $U$, of a structure is inversely related to the square of the structure's frequency.

To this end, the implicit frequency constraints given in Eq. (11b) can therefore be transformed into an explicit energy design constraint in terms of the sizing design variables as follows:

$$U_j(a_i) = \sum_{i=1}^{N} \left( \frac{e_{ij}}{a_i} + e'_{ij} \right) \le U_j^U \qquad (j = 1, 2, \ldots, M) \tag{16}$$

where the targeted strain energy threshold, $U_j^U$, can be obtained from

$$U_j^U = (n_{jo}/n_j^L)^2 (U_{jo}) \tag{17}$$

in which $n_{jo}$ is the $j$th mode natural frequency of the initial structure; $n_j^L$ is the minimum frequency target; and $U_{jo}$ is the calculated total internal energy of the initial structure.

## 5. The Optimality Criteria algorithm and design procedure

With the explicit formulation of the equivalent frequency constraints in Eq. (16), one can then proceed to solve the optimal element sizing design problem subject to the frequency constraints stated in Eqs. (11a)–(11c). The methodology for the solution of the optimal design problem is based on the Optimality Criteria (OC) approach, which has been shown to be highly efficient for large-scale structures with relatively few design constraints [14–17]. In this approach, a set of necessary optimality criteria for the optimal design is first derived and a recursive algorithm is then applied to indirectly search for the optimal solution by satisfying the derived optimality criteria.

### 5.1. Derivation of optimality criteria

In classical optimization theory, the necessary optimality criteria for the constrained optimization problem can be obtained by first converting the constrained problem to an unconstrained Lagrangian function and then solving for the stationary conditions of the Lagrangian function. By temporarily ignoring the sizing constraints in Eq. (11c), the unconstrained Lagrangian function, $L$, can be written as

$$L(a_i, \lambda_j) = \sum_{i=1}^{N} w_i\, a_i + \sum_{j=1}^{M} \lambda_j \left[ \sum_{i=1}^{N} \left( \frac{e_{ij}}{a_i} + e'_{ij} \right) - U_j^U \right] \tag{18}$$

where $\lambda_j$ denotes the Lagrange multiplier corresponding to the $j$th frequency constraint.

By differentiating the Lagrangian function in Eq. (18) with respect to the design variable, $a_i$, and setting the derivatives to zero, the necessary stationary conditions for the design optimization problem can be obtained from

$$\frac{\partial L(a_i, \lambda_j)}{\partial a_i} = w_i - \sum_{j=1}^{M} \lambda_j \left( \frac{e_{ij}}{a^2} \right) = 0 \quad (i = 1, 2, \ldots, N). \tag{19}$$

Rearranging the terms in Eq. (19) leads to the necessary optimality criteria:

$$\sum_{j=1}^{M} \lambda_j \left( \frac{e_{ij}}{w_i a_i^2} \right) = 1 \qquad (i = 1, 2, \ldots, N). \tag{20}$$

### 5.2. The recursive design algorithm

Based on the derived optimality criteria expressed in Eq. (20), a linear recursive relation to resize the active design variable, $a_i$, can be given as:

$$a_i^{\nu+1} = a_i^{\nu} \left[ 1 + \frac{1}{\eta} \left( \sum_{j=1}^{M} \frac{\lambda_j e_{ij}}{w_i a_i^2} - 1 \right)_{\nu} \right] \tag{21}$$

where $\nu$ denotes the current iteration number and $\eta$ is a relaxation parameter that controls the rate of convergence of the recursive process.

Before Eq. (21) can be used to find the design variable, $a_i$, the Lagrange multipliers, $\lambda_j$, must first be determined. By considering the sensitivity of the $k$th constraint due to the change in the design variable, $a_i$, the following simultaneous equations can then be established to solve for the set of Lagrange multipliers:

$$\sum_{j=1}^{M} \lambda_j^{\nu} \sum_{i=1}^{N} \left( \frac{e_{ik} e_{ij}}{w_i a_i^3} \right)_{\nu} = \sum_{i=1}^{N} \left( \frac{e_{ik}}{a_i} \right)_{\nu} - \eta (U_k^U - U_k^{\nu}) \quad (k = 1, 2, \ldots, M). \tag{22}$$

By successively applying Eqs. (21) and (22) until the convergence of $a_i$ as well as $\lambda_j$ occurs, the continuous optimal solution for the design problem subject to multiple frequency

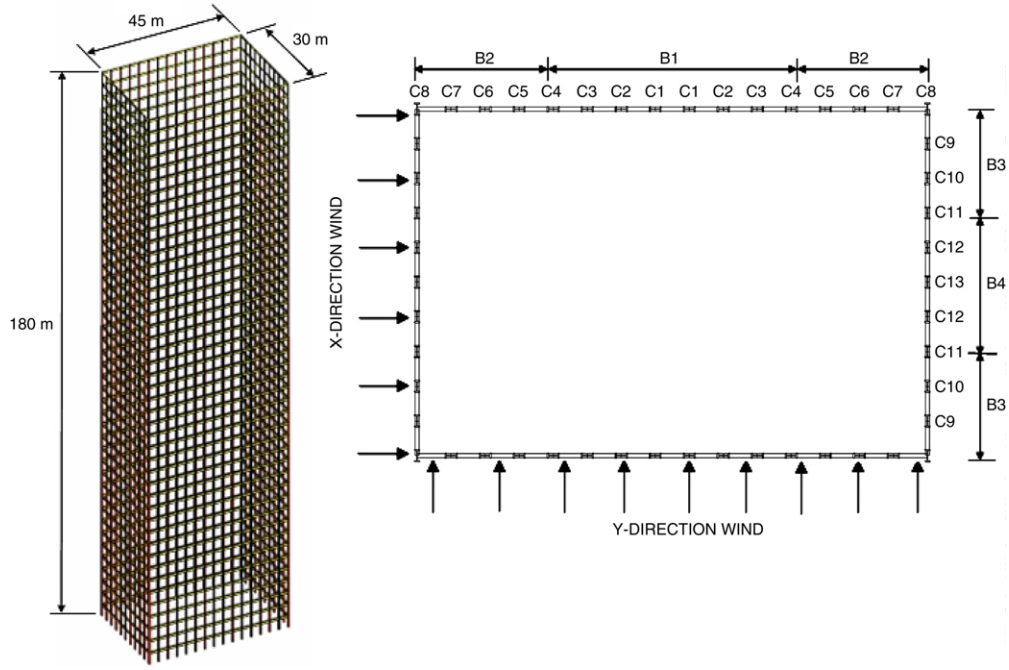


Fig. 2. 45-story steel building framework example with beam (B) and column (C) grouping.

constraints is found. When the optimal set of continuous cross-sectional area is obtained, it is necessary to finalize the design with discrete standard steel sections for practical use. A pseudo-discrete OC technique [17] can be used to achieve a smooth transition from the continuous variable design to the final discrete variable design using commercial standard steel sections.

### 5.3. Design procedure

The proposed integrated wind tunnel analysis and design optimization procedure is outlined step by step as follows:

1. Determine the aerodynamic force spectra from measured wind tunnel test data for a building structure.
2. Establish the alongwind and crosswind acceleration response functions using Eq. (5).
3. Balance the acceleration response function with the threshold acceleration criterion of ISO Standard 6897 in Eq. (10) to determine the set of minimum frequency targets.
4. Set up the finite element model for the building structure and carry out a dynamic analysis of the initial structure to determine the initial dynamic properties (i.e., modal frequencies, mode shapes, modal mass and stiffness) of the structure.
5. Establish minimum element sizes based on code specified strength design requirements.
6. Calculate the modal inertia loads and apply these loads statically to the structure. Carry out static analysis and establish the explicit frequency constraints of Eq. (16) expressed in the form of an energy formulation in terms of element sizing design variables.
7. Apply the recursive Optimality Criteria algorithm using Eqs. (21) and (22) to resize the elements of the structure until convergence of the element sizes and the values of Lagrange multipliers is achieved.
8. Repeat steps 6 and 7 for statically indeterminate structures until the cost of the structure between two successive reanalysis-and-redesign cycles converges to be within certain acceptable convergence criteria.
9. Apply the pseudo-discrete OC technique to finalize the optimal element sizes of the structure using discrete standard steel section.

## 6. Illustrative example: A 45-story tubular steel framework

A 45-story rectangular tubular steel building framework is used to illustrate the effectiveness of the proposed optimization design method. The external geometry and the member fabrication groupings of the symmetric framework are shown in Fig. 2. A story mass of 675,000 kg is lumped at the geometric centre of each floor level. Provided that solid floor slabs with relatively large axial stiffness are used in the building, all joints on the same floor level are assumed to move together as if on a rigid plate. All structural elements are to be designed using AISC standard steel sections as follows: W24 shapes for beams and W14 shapes for columns. For ease of construction, the columns on each vertical column line, the corner beams and the interior beams of the tube are grouped together to have a common section over three adjacent stories. The initial sizes have been taken to be W14 $\times$ 311 for columns and W24 $\times$ 176 for beams based on a preliminary strength check on their most critical members at the base of the framework. The initial first mode frequency is found to be 0.149 Hz in the Y-direction (short direction) of the building and the second mode frequency is 0.190 Hz in the X-direction (long direction) of the building.

Table 1
Wind-induced acceleration responses of the example building (m/s$^2$)

| | X-direction wind | | Y-direction wind | |
|---|---|---|---|---|
| | Alongwind | Crosswind | Alongwind | Crosswind |
| Before optimization | | | | |
| RMS Acceleration | 0.0313 | 0.0778 | 0.0549 | 0.0538 |
| ISO Standard 6897 | 0.0513 | 0.0567 | 0.0567 | 0.0513 |
| After optimization | | | | |
| RMS Acceleration | 0.0302 | 0.0502 | 0.0404 | 0.0502 |
| ISO Standard 6897 | 0.0503 | 0.0504 | 0.0504 | 0.0503 |

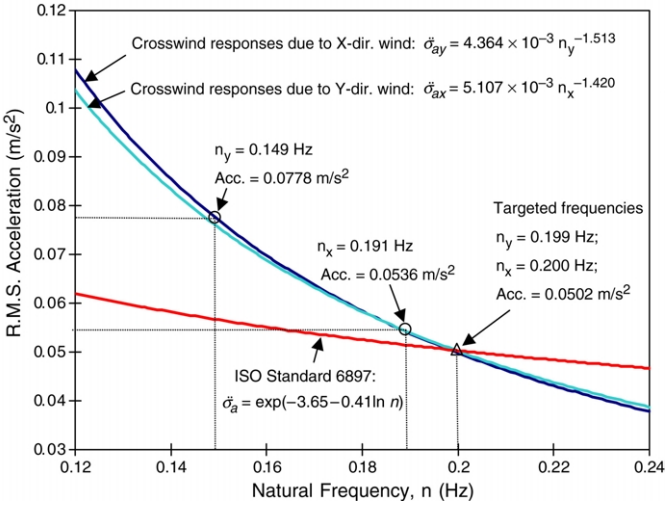


Fig. 3. Determination of targeted frequencies thresholds.

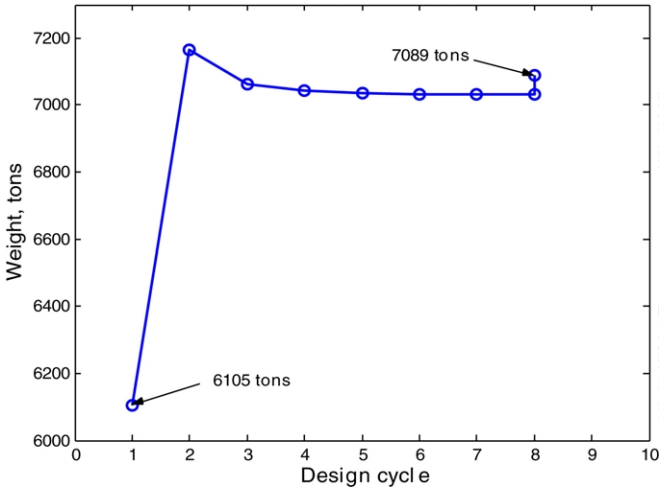


Fig. 4. Design history of structure weight.

### 6.1. Preliminary performance analysis of the example building

Since the example building has adopted the same geometrical shape of the CAARC standard building, one can utilize the previously established wind-tunnel-derived acceleration response functions given in Eqs. (8) and (9) to predict both the alongwind and crosswind acceleration performance of the example building. As shown in Table 1, while the alongwind acceleration responses of the building are found acceptable, the crosswind acceleration under either the X- or Y-direction wind is found to exceed the ISO Standard 6897 acceptability criteria. As a result, one has to consider suppressing the excessive vibration by enhancing the building's stiffness.

Based on the acceleration response functions given in Eqs. (8) and (9) and the ISO Standard 6897 criteria in Eq. (10), the minimum frequency targets in the two respective directions of the building are established. It has been found that the minimum first mode frequency target in the short direction of the building, $n_y^L$, should be 0.199 Hz while the second mode frequency target in the long direction, $n_x^L$, is 0.200 Hz as shown in Fig. 3. The fact that the two target frequencies for the example building are almost equal to 0.20 Hz is just coincidental. In general, a building may have different target frequency values for different modes of vibration.

### 6.2. Results and discussion

The design history of total tonnage of structural steel material is given in Fig. 4. Rapid and steady solution convergence is found within eight design cycles in which the structural steel tonnage is within 0.5% difference for the last five consecutive design cycles. The total steel tonnage of the structure is increased from 6105 tons to 7089 tons in order to stiffen the structure to achieve the desired minimum frequency targets. In order to demonstrate the effectiveness of the optimal design method, one may compare the optimal design results with those produced by the conventional simple scaling method. When using the simple scaling method to stiffen the structure to increase the first mode frequency from initially 0.149 Hz to the desired minimum frequency threshold of 0.199 Hz, the required total steel tonnage of the structure will be increased to

$$6105(0.199/0.149)^2 = 10{,}890 \text{ ton.} \quad (23)$$

As compared to the simple scaling method, the proposed optimization design method has achieved a significant saving of about 35% in materials.

Before optimization, the initial framework was found to have significant violations in crosswind acceleration when subject to lateral wind actions approaching from both the long and short directions of the building. Using the proposed optimization technique, the framework was successfully adjusted to the set of

Table 2
Final section sizes of the tubular frame example

| Storey no. | Column sizes | | | | | | | | | | | | | Beam sizes | | | |
|---|---|---|---|---|---|---|---|---|---|---|---|---|---|---|---|---|---|
| | C1 | C2 | C3 | C4 | C5 | C6 | C7 | C8 | C9 | C10 | C11 | C12 | C13 | B1 | B2 | B3 | B4 |
| 1–3 | W14×311 | W14×311 | W14×311 | W14×311 | W14×311 | W14×311 | W14×665 | W14×730 | W14×730 | W14×730 | W14×398 | W14×311 | W14×311 | W24×250 | W24×408 | W24×492 | W24×279 |
| 4–6 | W14×311 | W14×311 | W14×311 | W14×311 | W14×311 | W14×311 | W14×550 | W14×730 | W14×730 | W14×665 | W14×500 | W14×426 | W14×311 | W24×306 | W24×408 | W24×492 | W24×450 |
| 7–9 | W14×311 | W14×311 | W14×311 | W14×311 | W14×311 | W14×311 | W14×455 | W14×730 | W14×665 | W14×605 | W14×550 | W14×550 | W14×311 | W24×306 | W24×408 | W24×492 | W24×492 |
| 10–12 | W14×257 | W14×257 | W14×257 | W14×257 | W14×283 | W14×311 | W14×426 | W14×665 | W14×605 | W14×605 | W14×550 | W14×605 | W14×257 | W24×279 | W24×408 | W24×492 | W24×492 |
| 13–15 | W14×257 | W14×257 | W14×257 | W14×257 | W14×257 | W14×283 | W14×370 | W14×550 | W14×550 | W14×550 | W14×500 | W14×605 | W14×257 | W24×279 | W24×370 | W24×492 | W24×492 |
| 16–18 | W14×257 | W14×257 | W14×257 | W14×257 | W14×257 | W14×257 | W14×342 | W14×455 | W14×455 | W14×550 | W14×500 | W14×605 | W14×257 | W24×306 | W24×335 | W24×492 | W24×492 |
| 19–21 | W14×211 | W14×211 | W14×233 | W14×233 | W14×257 | W14×283 | W14×311 | W14×426 | W14×426 | W14×500 | W14×500 | W14×605 | W14×176 | W24×250 | W24×335 | W24×492 | W24×492 |
| 22–24 | W14×211 | W14×211 | W14×211 | W14×233 | W14×233 | W14×257 | W14×283 | W14×342 | W14×370 | W14×426 | W14×426 | W14×550 | W14×176 | W24×250 | W24×306 | W24×450 | W24×492 |
| 25–27 | W14×193 | W14×211 | W14×211 | W14×211 | W14×211 | W14×211 | W14×257 | W14×283 | W14×283 | W14×426 | W14×426 | W14×550 | W14×176 | W24×250 | W24×279 | W24×408 | W24×450 |
| 28–30 | W14×193 | W14×193 | W14×193 | W14×176 | W14×176 | W14×176 | W14×193 | W14×257 | W14×233 | W14×342 | W14×398 | W14×500 | W14×145 | W24×229 | W24×229 | W24×335 | W24×408 |
| 31–33 | W14×176 | W14×176 | W14×159 | W14×159 | W14×145 | W14×159 | W14×176 | W14×211 | W14×193 | W14×283 | W14×342 | W14×426 | W14×159 | W24×176 | W24×207 | W24×279 | W24×370 |
| 34–36 | W14×132 | W14×132 | W14×132 | W14×132 | W14×132 | W14×132 | W14×145 | W14×176 | W14×176 | W14×233 | W14×257 | W14×398 | W14 × 99 | W24×146 | W24×162 | W24×250 | W24×279 |
| 37–39 | W14×82 | W14×82 | W14×90 | W14×99 | W14×109 | W14×120 | W14×132 | W14×145 | W14×132 | W14×193 | W14×211 | W14×257 | W14×90 | W24×84 | W24×146 | W24×192 | W24×176 |
| 40–42 | W14×61 | W14×61 | W14×61 | W14×61 | W14×61 | W14×68 | W14×74 | W14×145 | W14×90 | W14×132 | W14×132 | W14×159 | W14×61 | W24×55 | W24×84 | W24×131 | W24×103 |
| 43–45 | W14×34 | W14×34 | W14×34 | W14×30 | W14×30 | W14×30 | W14×34 | W14×34 | W14×48 | W14×61 | W14×61 | W14×74 | W14×34 | W24×55 | W24×55 | W24×55 | W24×55 |

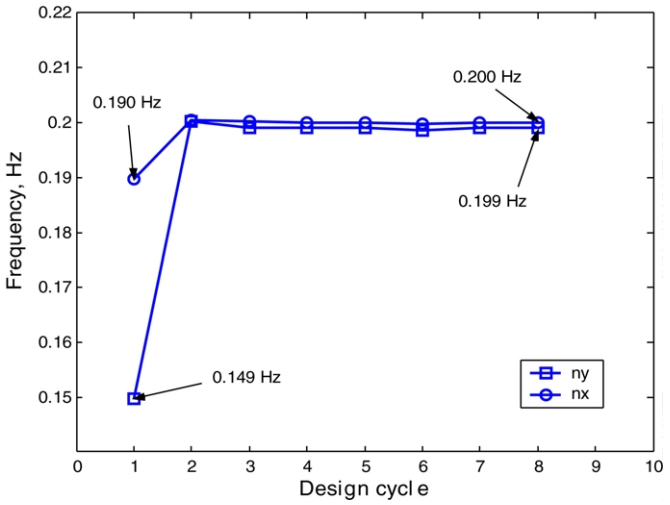


Fig. 5. Design history of modal frequencies.

derived frequencies. Indeed, the developed resizing technique is capable of searching for the optimal distribution of element stiffness in the structure to achieve simultaneously the first two targeted natural frequencies at 0.199 Hz and 0.200 Hz, respectively. As can be observed in Fig. 5, rapid convergence to the optimized structure with the targeted frequencies can be achieved generally in a few design cycles. Upon reaching the set of targeted frequencies, the crosswind RMS acceleration of the optimized structure is found to drop from 0.0778 $m/s^2$ to 0.0502 $m/s^2$, a reduction of 35.5%, when subject to the X-direction wind loading and from 0.0538 $m/s^2$ to 0.0502 $m/s^2$, a reduction of 6.7%, in the case of the Y-direction wind loading, indicating acceptable wind-induced responses attained simultaneously for the two wind loading conditions according to the ISO Standard 6897 occupant comfort criteria (see Table 1).

Due to symmetry, only the optimized discrete steel sections for one-quarter of the structural members of the framework are given in Table 2. A close scrutiny of the distribution of the element sizes indicates that the largest sections are found at the lowest base level, which is the most effective location to resist overturning moments. Moreover, larger section sizes on each floor are generally found at the corner columns and beams than on the columns and beams at the center of each frame. This can be explained by the fact that stiffer corner members can ensure effective tubular frame behavior by reducing the shear lag effects. As a result, the optimal element stiffness distributed achieved by the optimization method matches closely with sound engineering intuition and experience.

## 7. Concluding remarks

This paper has presented an integrated wind-induced vibration analysis and optimal resizing technique for element stiffness design of tall steel building structures subject to occupant comfort serviceability design criteria. Wind-induced vibrations have been successfully controlled by optimally resizing the structural elements to appropriately stiffen the building structure to meet a set of targeted frequencies derived from aerodynamic wind tunnel analysis and the motion perception design criteria of ISO Standard 6897. Encouraging results have been obtained in a full-scale 45-story symmetric tubular steel building framework with uncoupled wind-induced motions. Results indicate that rapid convergence to the optimal design of tall building structures is generally achieved in a few design cycles. It is envisaged that the methodology developed here can be further extended to the design of asymmetric tall building structures with complex mode shapes.

## Acknowledgments

This work was sponsored by the Research Grants Council of Hong Kong under project number HKUST6241/99E and is based upon research conducted by the second author under the supervision of the first author for the degree of Master of Philosophy in Civil Engineering at The Hong Kong University of Science and Technology. The authors are grateful to Dr. Peter Hitchcock and Professor Kenny C.S. Kwok of the CLP Power Wind/Wave Tunnel Facility at Hong Kong University of Science and Technology for their valuable assistance and suggestions throughout the course of this research work.

## References

[1] Chen PW, Robertson LE. Human perception thresholds of horizontal motion. Journal of Structural Engineering ASCE 1972;98:1681–95.
[2] Tallin A, Ellingwood B. Serviceability limit states: Wind induced vibrations. Journal of Structural Engineering ASCE 1983;110:2424–37.
[3] Griffis LG. Serviceability limit states under wind load. Engineering Journal AISC 1993;1st Qtr:1–16.
[4] Tschanz T, Davenport AG. The base balance technique for the determination of dynamic wind loads. Journal of Wind Engineering and Industrial Aerodynamics 1983;13:429–39.
[5] Zhou Y, Kijewski T, Kareem A. Aerodynamic loads on tall buildings: An interactive database. Journal of Structural Engineering ASCE 2003;129: 394–404.
[6] Cermak JE. Wind-tunnel development and trends in applications to civil engineering. Journal of Wind Engineering and Industrial Aerodynamics 2003;91:355–70.
[7] Kwok KCS, Bailey PA. Aerodynamic devices for tall buildings and structures. Journal of Engineering Mechanics ASCE 1987;113:349–65.
[8] Kwok KCS. Effect of building shape on wind-induced response of tall buildings. Journal of Wind Engineering and Industrial Aerodynamics 1988;28:381–90.
[9] Kwok KCS, Samali B. Performance of tuned mass dampers under wind loads. Engineering Structures 1995;17:655–67.
[10] Samali B, Kwok KCS. Use of viscoelastic dampers in reducing wind- and earthquake-induced motion of building. Engineering Structures 1995;17: 639–54.
[11] Spencer Jr BF, Nagarajaiah S. State of the art of structural control. Journal of Structural Engineering, ASCE 2003;129:845–56.
[12] Tamura Y. Design issues for tall buildings from accelerations to damping. In: Proceedings of 11th international conference on wind engineering. 2003.
[13] Venkayya VB. Optimality Criteria: a basic multidisciplinary design optimization. Computational Mechanics 1989;5:1–21.
[14] Chan CM, Grierson DE, Sherbourne AN. Automatic optimal design of tall steel building frameworks. Journal of Structural Engineering ASCE 1995; 121:838–47.
[15] Chan CM. Optimal lateral stiffness design of tall buildings of mixed steel and concrete construction. Journal of the Structural Design of Tall Buildings 2001;10:155–77.

[16] Chan CM. How to optimize tall steel building framework. In: Guide to structural optimization, ASCE manuals and report on engineering practice. 1997. p. 165–96.
[17] Chan CM. An optimality criteria algorithm for tall buildings design using commercial standard sections. Journal of Structural Optimization 1992;5: 26–9.
[18] Guidelines for the evaluation of the response of occupants of fixed structures to low frequency horizontal motion (0.063 to 1 Hz). ISO Standard 6897 1984, International Organization of Standardization.
[19] Kareem A. Wind-excited response of buildings in higher modes. Journal of Structural Engineering ASCE 1981;107:701–6.
[20] Chen X, Kareem A. Coupled dynamic analysis and equivalent static wind loads on buildings with three dimensional modes. Journal of Structural Engineering, ASCE 2005;131(7):1071–82.
[21] Kijewski T, Kwon DK, Kareem A. E-technologies for wind effects on structures. In: Proceedings of 11th international conference on wind engineering. 2003.
[22] Islam MS, Ellingwood B, Corotis RB. Dynamic response of tall buildings to stochastic wind load. Journal of Structural Engineering ASCE 1991; 116:2982–3002.
[23] Vickery BJ, Isyumov N, Davenport AG. The role of damping, mass and stiffness in the reduction of wind effects on structures. Journal of Wind Engineering and Industrial Aerodynamics 1983;11:285–94.
[24] Australian/New Zealand Standard (AS). Structural design actions part 2: wind actions, AS/NZS 1170.2:2002.
[25] Architectural Institute of Japan. AIJ recommendations for loads on buildings. 1996.
[26] Melbourne WH. Comparison of measurements on the CAARC standard tall building model in simulated model wind flows. Journal of Wind Engineering and Industrial Aerodynamics 1980;6:73–88.